Synthesis and Characterization of Highly Luminescent Asymmetric Poly(*p*-phenylene vinylene) Derivatives for Light-Emitting Diodes

Sung-Ho Jin,* Mi-Sun Jang, and Hong-Suk Suh

Department of Chemistry, Pusan National University, Pusan 609-735, Korea

Hyun-Nam Cho

Polymer Materials Lab, Korea Institute of Science and Technology, P.O.Box 131, Seoul 130-650, Korea

Ji-Hoon Lee

Polymer Lab, Samsung Advanced Institute of Technology, Taejon, Korea

Yeong-Soon Gal

Polymer Chemistry Lab, Central of General Education, Kyungil University, Hayang 712-701, Korea

Received June 20, 2001. Revised Manuscript Received October 15, 2001

Asymmetric and color tunable poly(*p*-phenylene vinylene) (PPV) derivatives with a dimethyldodecylsilylphenyl pendant group, poly[2-(3′-dimethyldodecylsilylphenyl)-1,4-phenylene vinylene] (*m*-SiPhPPV) and poly[2-(3′-dimethyldodecylsilylphenyl)-1,4-phenylene vinylene-*co*-2-methoxy-5-(2′-ethylhexyl oxy)-1,4-phenylene vinylene] (*m*-SiPhPPV-*co*-MEH−PPV), have been synthesized by a dehydrohalogenation method. Newly synthesized, these homo- and copolymers are highly soluble in common organic solvents. The defect-free uniformly thin films easily formed onto the indium tin oxide (ITO) coated glass substrate. The resulting polymers had high molecular weights with narrow polydispersities and high thermal stability up to 400 °C. The copolymers showed better optical and electroluminescent (EL) properties than those of the homopolymer. Single-layer light-emitting devices with an ITO/polymer/Al:Li alloy configuration were fabricated by using the resulting polymers. The maximum EL emissions of *m*-SiPhPPV and *m*-SiPhPPV-*co*-MEHPPV with various monomer feed ratios were observed at 528 and 588−595 nm, respectively. The emission color of the resulting polymers changed from green to orange. The EL properties of the *m*-SiPhPPV-*co*-MEH−PPV dramatically improved compared to those of *m*-SiPhPPV and MEH−PPV. The maximum brightness and the external luminance efficiency of the *m*-SiPhPPV-*co*-MEH−PPV were up to 19 180 cd/m^2 and 2.9 lm/W. The half lifetime of a single-layer device at 1000 cd/m^2 is about 120 h.

Introduction

Organic electroluminescent (EL)[1−6] diodes have attracted much attention because of their wide viewing angle and fast switching time as compared to conventional displays, liquid-crystal displays (LCDs), and their potential application for large-area flat panel displays that can be driven at low voltage. Since Tang and VanSlyke demonstrated a high-efficiency EL diode consisting of light-emitting layers and carrier transport layers,[1,7] various kinds of electroluminescent polymers as well as organic fluorescent dyes have been developed to obtain high efficiency, long lifetime, and even white-color emission materials for LCD backlight.[8]

Conjugated polymer-based EL diodes appear to be very promising for the development of low-cost, multicolored, large-area flat panel display because of the feasible design of the molecular structures.[9,10] However, there are a number of impediments remaining that need

* To whom correspondence should be addressed: E-mail shjin@hyowon.pusan.ac.kr. Fax: +82-51-581-2348.

(1) Tang, C. W.; VanSlyke, S. A. *Appl. Phys. Lett.* **1987**, *51*, 913.
(2) Tang, C. W.; VanSlyke, S. A.; Chen, C. H. *J. Appl. Phys.* **1989**, *65*, 3610.
(3) Adachi, C.; Tsutsui, T.; Saito, S. *Appl. Phys. Lett.* **1990**, *56*, 799.
(4) Burroughes, J. H.; Bradley, D. D. C.; Brown, A. R.; Marks, R. N.; Mackay, K.; Friend, R. H.; Burns, P. L.; Holmes, A. B. *Nature* **1990**, *347*, 539.
(5) Ohmori, Y.; Uchida, M.; Muro, K.; Yoshino, K. *Jpn. J. Appl. Phys.* **1991**, *30*, L1938.
(6) Braun, D.; Heeger, A. J. *Appl. Phys. Lett.* **1991**, *58*, 1982.
(7) VanSlyke, S. A.; Bryan, P. S.; Tang, C. W. *Proceedings of the 8th International Workshop on Inorganic and Organic Electroluminescence*, Berlin, Germany, 1996; p 195.
(8) Kido, J.; Shionoya, H.; Nagai, K. *Appl. Phys. Lett.* **1995**, *67*, 2281.
(9) Mitschke, U.; Bäuerle P. *J. Mater. Chem.* **2000**, *10*, 1471.
(10) Kraft, A.; Grimsdale, C.; Holmes, A. B. *Angew. Chem., Int. Ed.* **1998**, *37*, 402.

10.1021/cm010593s CCC: $22.00
Published on Web 01/09/2002

to be resolved for commercialization. For example, many organic and polymer-containing diodes have low EL efficiencies, deficient color-control capabilities, and very short operating lifetimes and are unstable in the open air.

Various techniques have been proposed to improve the efficiency of the device by modifying the chemical structure of the polymer with bulky phenyl side groups, or PPV-based (poly(*p*-phenylene vinylene)-based) alternating copolymers containing conjugated phenylenevinylene segments and nonconjugated spacers.[11−13] These bulky side groups interrupt conjugation and interfere with the packing of the polymer chain, which results in the formation of amorphous PPVs. Another method to improve the efficiency of the devices is the blending system using hole-transporting and electron-transporting materials to balance the injected charges.[14−16] However, the use of a polymer blending system in a polymer LED caused some phase separation during the long operation time of the device, which could be detrimental to the device's performance. Among the conjugated polymers, PPVs and their derivatives are known as the most promising materials for the application of polymer LEDs. These materials have been synthesized by precursor routes or the dehydrohalogenation method, leading to soluble and high molecular weight polymers. In our previous works, we have synthesized various types of novel EL polymers and blending systems with an electron transport polymer containing an oxadiazole repeating unit to improve the efficiency as well as to control the color tuning of the polymers.[17−20] The EL properties of the blending system were improved as compared to the EL polymer itself.

In the present article, we report a new series of asymmetric and color-tunable PPV derivatives, including copolymers, that were developed to overcome the phase separation in polymer blending systems with MEH−PPV units, which were synthesized via the Gilch polymerization for high molecular weight, narrow polydispersity, and good thermal stability. To improve the EL efficiency, the bulky dimethyldodecylsilylphenyl group was introduced into the meta position of the phenyl substitutent, which inhibits the intermolecular interaction between the resulting polymer chains. The meta substitutent linkage also improves the amorphous state and processibility. To our knowledge, there have never been reports focused on improving device performance using membrane technology or molecular cutting experiments of the organic soluble EL polymers. We first report here highly purified polymeric EL materials by membrane dialysis, which improved the device performance.

Experimental Section

Materials. 1,3-Dibromobenzene, chlorododecyldimethylsilane, 2-bromo-*p*-xylene, *n*-butyllithium (1.6 M hexane solution), 1,3-[bis(diphenylphosphino)propane]dichloronickel(II) ($NiCl_2$(dppp)), magnesium granules, *N*-bromosuccinimide (NBS), and potassium *tert*-butoxide (1.0 M solution in THF) were purchased from Aldrich and used without further purification unless otherwise noted. Solvents were dried and purified by fractional distillation over sodium/benzophenone and handled in a moisture-free atmosphere. The moisture content of THF was below 10 ppm. Column chromatography was performed using silica gel (Merck, 250−430 mesh). The polyvinylidene fluoride dialysis membrane was purchased from Spectrum Co.

Synthesis of 1-Bromo-3-(dimethyldodecylsilyl)benzene (1). In a round-bottom flask were placed 1,3-dibromobenzene (4.62 g, 19 mmol) and dry THF (150 mL) under a N_2 atmosphere. The flask was cooled to −78 °C. While the solution was being stirred, *n*-BuLi (11.9 mL, 1.6 M *n*-hexane solution, 19 mmol) was added dropwise, causing a lightening of the yellow color. After being stirred for 1 h at −78 °C, the mixture was allowed to cool to room temperature and then stirred for an additional 1 h. After the mixture cooled to −78 °C, chlorododecyldimethylsilane (5.0 g, 19 mmol) was added dropwise, and the system was allowed to slowly warm to room temperature and stirred for an additional 3 h. Most of the solvent was evaporated under a reduced pressure. The crude product was further purified by vacuum distillation, resulting in a colorless liquid (bp 155 °C/0.8 mmHg, yield 74%). ^{1}H NMR ($CDCl_3$): δ 0.27 (s, 6H, $Si(CH_3)_2$, 0.77 (t, 2H, $SiCH_2$), 0.92 (t, 3H, $-CH_3$), 1.27 (m, 20H, $(CH_2)_{10}$), 7.21 and 7.49 (d, 4H, aromatic protons).

Synthesis of 1,4-Dimethyl-2-(3′-dimethyldodecylsilylphenyl)benzene (3). The Grignard reagent of *p*-xylene-2-magnesium bromide (**2**), prepared from the reaction of 2-bromo-*p*-xylene (8.04 g, 43.4 mmol) with Mg (1.56 g, 65 mmol) in 70 mL of dry THF, was added to a solution of 1-bromo-3-(dimethydodecylsilyl)benzene (**1**) (18.38 g, 54 mmol) in 100 mL of dry THF containing $NiCl_2$(dppp) (0.025 g, 0.1 mol %) as a catalyst. After refluxing for 18 h, the reaction mixture was quenched with 1 N HCl and poured into an excess of water and extracted with chloroform. The combined organic layers were washed with water two more times and then dried over anhydrous $MgSO_4$. After removal of the solvent, the residue was subjected to purification by chromatography on silica gel using hexane as an eluent (yield: 63%). ^{1}H NMR ($CDCl_3$): δ 0.31 (s, 6H, $Si(CH_3)_2$, 0.77 (t, 2H, $SiCH_2$), 0.93 (t, 3H, $-CH_3$), 1.56 (m, 20H, $(CH_2)_{10}$), 2.28 and 2.4 (s, 6H, $2CH_3$ on aromatic ring), 7.05−7.55 (m, 7H, aromatic protons).

Synthesis of 1,4-Bis(bromomethyl)-2-(3′-dimethyldodecylsilylphenyl)benzene (4). A mixture of 1,4-dimethyl-2-(3′-dimethyldodecylsilylphenyl)benzene (**3**) (10 g, 24.4 mmol), *N*-bromosuccinimide (11.25 g, 56 mmol), and benzoyl peroxide (12 mg, 0.05 mmol) in CCl_4 (200 mL) was heated to reflux for 12 h under a N_2 atmosphere. A bright red solution with precipitated succinimide was produced. The warm reaction mixture was filtered under suction and washed with a small amount of hot CCl_4. The combined organic layers were dried over anhydrous $MgSO_4$. After the solvent was removed, the residue was subjected to purification by chromatography on silica gel using hexane as an eluent (yield: 30%). ^{1}H NMR ($CDCl_3$): δ 0.29 (s, 6H, $Si(CH_3)_2$, 0.79 (t, 2H, $SiCH_2$), 0.91 (t, 3H, $-CH_3$), 1.31 (m, 20H, $(CH_2)_{10}$), 4.47 and 4.52 (s, 4H, $2\text{-}CH_2Br$), 7.29−7.62 (d, 7H, aromatic protons).

Synthesis of Poly[2-(3′-dimethyldodecylsilylphenyl)-1,4-phenylene vinylene-*co*-2-methoxy-5-(2′-ethylhexyloxy)-1,4-phenylene vinylene] (*m*-SiPhPPV-*co*-MEH−PPV). A solution of 6 mL of potassium *tert*-butoxide (1.0 M THF

(11) Sokolik, I.; Yang, Z.; Karasz, F. E.; Morton, D. C. *J. Appl. Phys.* **1993**, *74* (5), 3584.
(12) Yang, Z.; Karasz, F. E.; Geise, H. J. *Macromolecules* **1993**, *26*, 6570.
(13) Pasco, S. T.; Lahti, P. M.; Karasz, F. E. *Macromolecules* **1999**, *32*, 6933.
(14) Jin, S. H.; Jung, J. E.; Park, D. K.; Jeon, B. C.; Kwon, S. K.; Kim, Y. H.; Moon, D. K.; Gal, Y. S. *Eur. Polym. J.* **2001**, *37*, 921.
(15) Lee, S. H.; Jin, S. H.; Moon, S. B.; Song, I. S.; Kim, W. H.; Kwon, S. K.; Park, N. K.; Han, E. M. *Mol. Cryst. Liq. Cryst.* **2000**, *349*, 507.
(16) Jin, S. H.; Kim, W. H.; Song, I. S.; Kwon, S. K.; Lee, K. S.; Han, E. M. *Thin Solid Films* **2000**, *363* (12), 255.
(17) Jin, S. H.; Sun. Y. K.; Sohn, B. H.; Kim, W. H. *Eur. Polym. J.* **2000**, *36*, 957.
(18) Kim. D. J.; Kim, S. H.; Jin, S. H.; Park, D. K.; Cho, H. N.; Zyung, T.; Cho, I.; Choi, S. K. *Eur. Polym. J.* **1999**, *35*, 227.
(19) Kim, D. J.; Kim, S. H.; Zyung, T.; Kim, J. J.; Cho, I.; Choi, S. K. *Macromolecules* **1996**, *29*, 3657.
(20) Han, E. M.; Gu, H. B.; Kim, W. H.; Jin, S. H.; Lee, S. H.; Moon, S. B. *Mol. Cryst. Liq. Cryst.* **2000**, *349*, 467.

solution, 6 mmol) was slowly added to a stirred solution of monomer (**4**) (0.39 g, 0.75 mmol) and 1,4-bis(chloromethyl)-2-(2′-ethylhexyloxy)-5-methoxybenzene (0.084 g, 0.25 mmol) in 50 mL of dry THF over 1 h using a syringe pump that was cooled to −5 °C. The reaction mixture, which gradually increased its viscosity and its orange-red fluorescence, was stirred for 3 h. A small amount of 4-*tert*-butylbenzyl bromide was added to the mixture to end-cap the polymer chain and was further stirred for 1 h. The polymerization solution was poured into 600 mL of methanol and the crude polymer was Soxhlet-extracted with methanol to remove the impurities and oligomers. The resulting polymer was redissolved in chloroform and reprecipitated into methanol. After filtration and drying under a vacuum, a bright red polymer fiber, *m*-SiPhPPV-*co*-MEH−PPV, was obtained (0.52 g, 82%). ^{1}H NMR ($CDCl_3$): δ 0.28 (s, 6H, $Si(CH_3)_2$), 0.70−0.91 (m, 11H, $SiCH_2$ and $-CH_3$ ×3), 1.10−1.60 (m, 31H, methylene and methine protons), 3.8−4.2 (m, 5H, $-OCH_2$ and $-OCH_3$), 7.10−7.60 (br, 13H, aromatic protons and vinylic protons).

m-SiPhPPV was polymerized using a similar method for poly(*m*-SiPhPPV-*co*-MEH−PPV). ^{1}H NMR ($CDCl_3$): δ 0.30 (s, 6H, $Si(CH_3)_2$), 0.70−0.98 (m, 5H, $SiCH_2$ and $-CH_3$), 1.10−1.52 (m, 20H, $(CH_2)_{10}$), 7.10−7.80 (br, 9H, aromatic protons and vinylic protons). IR (KBr pellet, cm^{-1}): 3056, 3018, 2954, 2922, 2853, 1619, 1597, 1488, 1465, 1407, 1382, 1247, 1104, 1036, 1018, 962, 826, 773, 723, 698. Anal. Calcd for $C_{28}H_{40}Si$: C, 83.10; H, 9.96. Found: C, 82.90; H, 9.86.

Polymer Purification. The resulting polymers, *m*-SiPhPPV and *m*-SiPhPPV-*co*-MEH−PPV, were further purified using a polyvinylidene fluoride dialysis membrane to improve the device's performance. After the normal procedures of polymer purification, as mentioned above, were followed, the polymer solution in chloroform was dialyzed against chloroform solvent for 3 days or a week while stirring to remove the low and medium molecular weight polymer portions. After dialysis, the purified fibrous polymers were obtained by pouring them into 500 mL of methanol, filtered, and vacuum-dried.

Characterization. ^{1}H NMR spectra were recorded using a Bruker AM-300 spectrometer, and chemical shifts were recorded in ppm units with the residual proton solvent resonance as a reference (chloroform: 7.26 ppm). The UV−visible spectra were recorded on a Shimadzu UV-3100 spectrophotometer with baseline corrections and normalizations carried out using Microsoft Excel software. The FT-IR spectra were measured on a Nicolet DX-5B spectrometer in KBr pellets. The molecular weights and polydispersities of the polymers were determined by gel permeation chromatography (GPC) analysis relative to polystyrene calibration (Waters high-pressure GPC assembly Model M590 pump, μ-styragel columns of 10^5, 10^4, 10^3, 500, and 100 Å, refractive index detectors) in a THF solution. Thermal analyses were carried out on a Dupont TGA 9900 thermogravimetric analyzer under a nitrogen atmosphere at a rate of 10 °C/min. Emission spectra were made on a dilute ($\sim 10^{-6}$ M) solution collected on a Perkin-Elmer LS-50 fluorometer utilizing a lock-in amplifier system with a chopping frequency of 150 Hz. Solid-state emission measurements were achieved using film supported on a glass substrate and mounted with front-face excitation at an angle of <45°. Ultraviolet photoelectron spectroscopy (UPS) was performed using a VG ESCA LAB MKII spectrometer. The occupied electronic states were measured with HeI radiation ($h\nu = 21.2$ eV). The absolute binding energy of the occupied states versus vacuum was measured according to the method described by Schmidt et al.[21] The polymer film was excited with several portions of visible light from a xenon lamp. To measure EL, a polymer light-emitting diode was constructed as follows: The glass substrate coated with a transparent ITO electrode was thoroughly cleaned by successive ultrasonic treatments in acetone, isopropyl alcohol, and distilled water, dried with nitrogen gas, and heated for drying. The polymer film was prepared by spin casting a polymer solution containing 0.5 wt % of toluene (or chloroform). Uniform and pinhole-free films with a thickness around 120 nm were easily obtained from the resulting polymer solution. Metal contact (Al:Li, 99.73:0.23%) was deposited on the top of the polymer film through a mask by vacuum evaporation at pressure below 4 × 10^{-6} Torr, yielding active areas of 4 mm^2. For the measurements of device characteristics, current−voltage ($I-V$) changes were measured using a current/voltage source (Keithley 238) and an optical power meter (Newport 818-SL). All processes and measurements mentioned above were carried out in the open air at room temperature.

Results and Discussion

Monomer and Polymer Synthesis. Scheme 1 outlines the synthesis and polymerization of the asymmetric monomer **4**, 1,4-bis(bromomethyl)-2-(3′-dimethyldodecylsilylphenyl)benzene, *m*-SiPhPPV, and copolymers, *m*-SiPhPPV-*co*-MEH−PPVs, with various monomer feed ratios. The newly designed monomer **4** was prepared in a four-step reaction. The 1-bromo-3-(dimethyldodecylsilyl)benzene was produced by the reaction of 1-lithio-3-bromobenzene, which was generated by the addition of *n*-butyllithium to 1,3-dibromobenzene at −78 °C, with chlorododecyldimethylsilane in high yield (74%). The reaction of 1,4-dimethyl-2-phenylmagnesium bromide and compound **1** through nickel-catalyzed Grignard coupling reaction produced compound **3**. Compound **3** was further reacted with *N*-bromosuccinimide (NBS) in the presence of a catalytic amount of benzoyl peroxide to afford monomer **4**. The overall yield of the reactions was about 14% because of the low yield of the bromination step. The MEH−PPV monomer **5** was prepared as described earlier.[22]

The key intermediate in this synthesis is the introduction of bent-type dodecyldimethylsilylphenyl substitutent into the phenylene unit. The insertion of a long-chain dodecyldimethylsilylphenyl group as the side chain of a PPV backbone yields unique properties, which include good flexibility, solubility, adhesion to the substrate and electrodes, and improved device performances. Another advantage of using the silicon atom is the effective introduction of various substitutents, such as linear long-chain alkyl or branched and perfluorinated alkyl groups. The effects of silicon substitutents on the luminescence properties of a PPV-based polymer has been reported.[23] Also, by the introduction of a bulky substitutent to the proper position in the phenylenevinylene's backbone, one can control the effective conjugation length, the tunability of the emission colors, and the packing density of the polymer chains. This results in the formation of amorphous PPVs and a more highly efficient device performance than the ordered crystalline PPV derivatives.

The homopolymerization of monomer **4** and the copolymerization with 1,4-bis(chloromethyl)-2-(2,-ethylhexyloxy)-5-methoxybenzene were performed with an excess of potassium *tert*-butoxide in THF cooled in an ice water bath under a N_2 atmosphere. When polymerization was carried out with the Gilch polymerization method, most of the phenyl-substituted PPVs were produced as homogeneous soluble portions together with

(21) Schmidt, A.; Armstrong, N. R.; Goeltner, C.; Mullen, K. *J. Phys. Chem.* **1994**, *98*, 11780.

(22) Wudl, F.; Srdanov, G. U.S. Patent No. 5189136, 1993.

(23) Chuah, B.; Hwang, D. H.; Kim, S. T.; Moratti, S. C.; Holmes, A. B.; Mello, J. C. D.; Friend, R. H. *Synth. Met* **1997**, *91*, 279.

Scheme 1

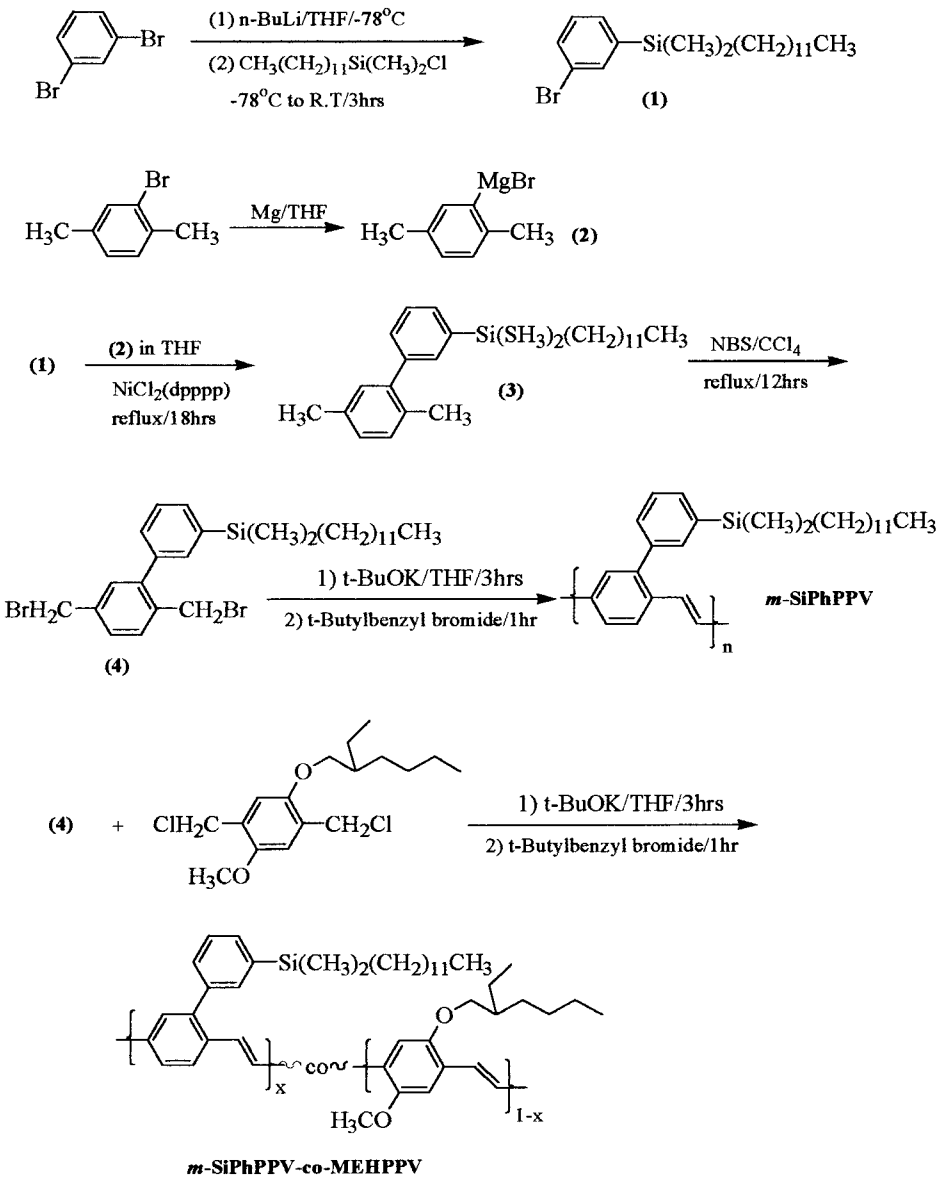

some insoluble gel portions. This limits their applications and makes it very difficult to control the polymerization behavior of PPV derivatives for mass production. During the polymerization of our monomer systems, however, the reaction mixture became progressively viscous as well as perfectly homogeneous without any precipitates. The resulting electroluminescence polymers, *m*-SiPhPPV, and copolymers were completely soluble in common organic solvents, such as chloroform, chlorobenzene, toluene, THF, and xylene.

Table 1 summarizes the polymerization results and molecular weights of the *m*-SiPhPPV, copolymers and MEH−PPV. The weight average molecular weights (M_w) and polydispersities of the *m*-SiPhPPV, copolymers, and MEH−PPV were found to be in the range of 2.7−9.6 × 10^5 and 1.86−3.40, respectively. The number average degree of polymerization was estimated to be $n \sim 430$ for *m*-SiPhPPV and $n \sim 840$ for *m*-SiPhPPV-*co*-MEH−PPV (75:25 wt %). To improve the color purity and the PL and EL efficiency, *m*-SiPhPPV, copolymers, and MEH−PPV were further purified by membrane technology. The polymer solution in chloroform was dialyzed against a chloroform solvent with a dialysis membrane made from PVDF for 3 days or a week to remove the medium molecular weight polymers (MWCO of 80 000 Da). The remaining solution in the dialysis membrane was poured into methanol, filtered, and dried under a vacuum. From these processes, highly purified *m*-SiPhPPV, copolymers, and MEH−PPV were obtained. After cutting off a medium molecular weighted portion

Table 1. Polymerization Results and Molecular Weights of *m*-SiPhPPV, Copolymers, and MEH−PPV before the Membrane Dialysis

polymers	M_w[a] × 10^5	PDI	yield (%)
m-SiPhPPV	9.6	3.40	75
m-SiPhPV-*co*-MEH−PPV (90:10 wt %)[b]	2.7	1.92	80
m-SiPhPV-*co*-MEH−PPV (75:25 wt %)[b]	8.3	2.0	82
m-SiPhPV-*co*-MEH−PPV (20:80 wt %)[b]	5.4	1.86	85
MEH−PPV	8.0	2.67	80

[a] GPC in THF using polystyrene standards. [b] Composition determined from ^{1}H NMR spectroscopy.

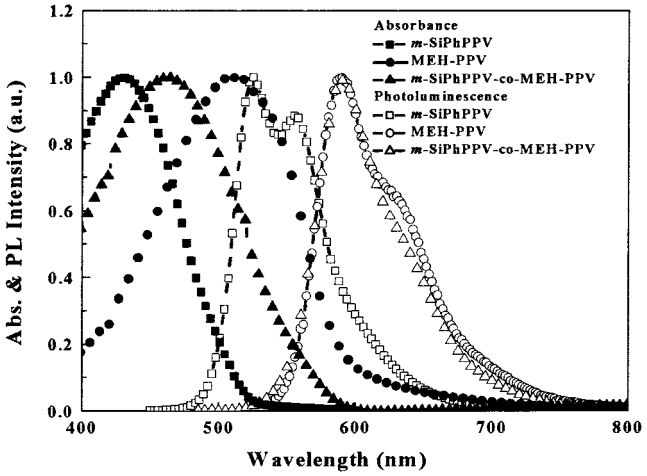

Figure 1. UV−visible absorption and photoluminescence spectra of *m*-SiPhPPV, *m*-SiPhPPV-*co*-MEH−PPV (75:25 wt %), and MEH−PPV in the solid state.

by using membrane technology, *m*-SiPhPPV, copolymers, and MEH−PPV exhibited the narrow polydispersity and sharp GPC curves. During the molecular cutting experiment, the M_w and polydispersity of *m*-SiPhPPV-*co*-MEH−PPV (75:25 wt %) values were changed from 8.3×10^5 and 1.69 to 10.3×10^5 and 1.60, respectively.

The structure of the *m*-SiPhPPV and copolymers was identified by ^{1}H NMR, FT-IR, and UV−visible spectroscopy. The disappearance of the characteristic benzylic proton peaks (4.45 and 4.50 ppm) of monomer **4** and the appearance of a new vinylic proton peak (7.10 ppm) with aromatic phenyl protons confirmed the complete polymerization. All other peaks showed good correspondence with the chemical structure of the polymers. The ^{1}H NMR spectrum of the copolymers showed a signal at 0.28 ppm for dimethyl groups on a silicon atom and at 3.8−4.2 ppm for methylene next to oxygen and methoxy groups in side chains. From the comparison of the peak areas at 0.28 and 3.8−4.2 ppm, the copolymers compositions were calculated. The composition of the present copolymers, *m*-SiPhPPV-*co*-MEH−PPVs, is about 90:10, 75:25, and 20:80 wt % with *m*-SiPhPPV and MEH−PPV units. The FT-IR spectrum of the polymer showed the expected absorptions at 962 and 3056 cm^{-1}, respectively, because of the C−H out-of-plane bending and stretching modes for the vinylene C=C bonds of trans configuration. The degradation pattern for the polymers under nitrogen is very simple. The TGA thermogram of the *m*-SiPhPPV-*co*-MEH−PPV (75:25 wt %) revealed a high thermal stability of up to 400 °C (5% weight loss at 406 °C), which means that deformation and degradation of the polymeric emitting layer from current-induced heat during operation of the EL device was prevented.[24]

Optical and Electroluminescence Properties. An optical-quality film could easily be cast onto an ITO coated-glass substrate for device fabrication. Figure 1 shows the optical absorption and the PL spectra of *m*-SiPhPPV, copolymers, and MEH−PPV thin films coated on a carboglass. The maximum absorption spectra of the *m*-SiPhPPV, *m*-SiPhPPV-*co*-MEH−PPV (75:25 wt %), and MEH−PPV thin films have a relatively sharp peak at 435, 464, and 510 nm with an onset of absorption at 535, 600, and 590 nm, respectively. These spectra in chloroform are almost identical except that the peak is broader for the solid film. The red shift of the maximum absorption in *m*-SiPhPPV-*co*-MEH−PPV (75:25 wt %) is probably due to the introduction of the MEH−PPV part and the extension of the polymer main chain. Absorption and PL maximum peaks of the copolymers were red-shifted at least 10 wt % of MEH−PPV parts in copolymer compositions. The absorption and emission maxima of the *m*-SiPhPPV, copolymers, and MEH−PPV are summarized in Table 2. The copolymers show an almost identical maximum of PL peaks with MEH−PPV. The external PL quantum efficiencies of MEH−PPV and *m*-SiPhPPV-*co*-MEH−PPV (75:25 wt %) in the solid state were measured by using the integrating sphere method.[25] According to the integrating sphere method, a value of 18 ± 2% for the external quantum efficiency of the MEH−PPV was obtained. The value of *m*-SiPhPPV-*co*-MEH−PPV (75:25 wt %) was determined to be as high as 21 ± 2%, which is higher than that of MEH−PPV. The higher external PL quantum efficiency of *m*-SiPhPPV-*co*-MEH−PPV (75:25 wt %) as compared to MEH−PPV is attributed to the bulky dimethyldodecylsilylphenyl group linked to the phenylene ring, which twists the backbones and inhibits the intermolecular interaction of the conjugated chains. The work function and the surface roughness of ITO have a crucial effect on the device's performance.

Table 2. Absorption, PL, and EL Data of *m*-SiPhPPV, Copolymers, and MEH−PPV

polymers	Abs_{max} (nm)	PL_{max} (nm)	EL_{max} (nm)
m-SiPhPPV	435	525	528
m-SiPhPV-*co*-MEH−PPV (90:10 wt %)	434	588	589
m-SiPhPV-*co*-MEH−PPV (75:25 wt %)	464	594	595
m-SiPhPV-*co*-MEH−PPV (20:80 wt %)	505	598	590
MEH−PPV	510	592	590

Most of the conjugated semiconducting polymers reach the HOMO level more than 5 eV below vacuum. So there is a significant energy barrier to hole injection into the polymer, which must be responsible for an increase in the amount of voltage needed to turn on the devices. To solve these problems and improve the luminance efficiency, many research groups have studied the insertion of hole-injection-transport layers, such as polyaniline (PANI) doped with camphor sulfonic acid (CAS) or poly(3,4-ethylenedioxythiophene) (PEDOT) doped with poly(styrenesulfonate) (PSS).[26,27] Isopropyl alcohol (10 wt %) was added to the PEDOT/PSS aqueous solution, and after filtration, PEDOT was spin-coated on the surface-treated ITO substrate and dried for 5 min at 110 °C to remove the residual solvent. The resulting emissive polymer solutions were successively spun on

(24) Tessler, N.; Harrison, N. T.; Thomas, D. S.; Friend, R. H. *Appl. Phys. Lett.* **1998**, *73*, 732.

(25) John, C.; Mello, C.; Winmann, F.; Friend, R. H. *Adv. Mater.* **1997**, *9*, (3), 230.

(26) Carter, S. A.; Scott, J. C.; Brock, P. J. *Appl. Phys. Lett.* **1997**, *71*, 1145.

(27) Karg, S.; Scott, J. C.; Salem, J. R.; Angelopoulos, M. *Synth. Met.* **1996**, *80*, 111.

the top of the PEDOT film. After that, the aluminum−lithium alloy was thermally evaporated at $\approx 10^{-6}$ mbar. The band gaps of *m*-SiPhPPV, *m*-SiPhPPV-*co*-MEH−PPV (75:25 wt %), and MEH−PPV (taken from the onset of the absorption spectrum) are 2.31, 2.06, and 2.10 eV, respectively. An energy band diagram for the *m*-SiPhPPV, *m*-SiPhPPV-*co*-MEH−PPV (75:25 wt %), and MEH−PPV was determined from optical absorption spectra and UPS by obtaining the energy gap and the ionization potential (IP) of the polymers. IP was determined by direct comparison to the UPS data obtained from the solution cast film of *m*-SiPhPPV, *m*-SiPhPPV-*co*-MEH−PPV (75:25 wt %), and MEH−PPV. The electron affinity (E_a) level was approximated by subtracting the optical band gap from the HOMO binding energy.

The emission spectra were obtained by the excitation of the polymers at the maximum absorption wavelength. The maximum emission peaks of the *m*-SiPhPPV, *m*-SiPhPPV-*co*-MEH−PPV (75:25 wt %), and MEH−PPV were observed at 525, 594, and 592 nm, which corresponded to green and orange-red light, respectively. The maximum PL spectrum of the *m*-SiPhPPV-*co*-MEH−PPV (75:25 wt %) is similar to that of MEH−PPV. This indicates that the copolymer systems energy transfer occurs from the *m*-SiPhPPV segment to the MEH−PPV part of the copolymers. The barrier heights were found to be 0.41, 0.25, and 0.4 eV at the interface of the Al:Li (3.4 eV)/LUMO state for the electron and 0.60, 0.51, and 0.40 eV at the interface of the ITO (4.7 eV)/HOMO state of the *m*-SiPhPPV, *m*-SiPhPPV-*co*-MEH−PPV (75:25 wt %), and MEH−PPV for the hole, respectively. Most of the EL polymers tend to be p-type semiconductors with a much greater tendency to transport holes than electrons.[28] These polymers showed that the major carrier is the hole rather than electron, although the band offset of Al:Li/LUMO is smaller than that of ITO/HOMO. The electron injection of *m*-SiPhPPV-*co*-MEH−PPV (75:25 wt %) is much easier than that of *m*-SiPhPPV and MEH−PPV.

These results strongly support the *I*−*V* characteristics and luminance efficiency of the *m*-SiPhPPV, *m*-SiPhPPV-*co*-MEH−PPV (75:25 wt %), and MEH−PPV. Figure 2 shows the hypothesized energy level diagram of the ITO/PEDOT/*m*-SiPhPPV/Al:Li (A), ITO/PEDOT/*m*-SiPhPPV-*co*-MEH−PPV (75:25 wt %)/Al:Li (B), and the ITO/PEDOT/MEH−PPV/Al:Li (C) devices fabricated in this work. Figure 3 shows the current−voltage−luminance characteristics of ITO/PEDOT/polymer/Al:Li devices. The amount of turn-on voltages of (A), (B), and (C) devices are 14, 2.3, and 2.0 V, respectively. The higher turn-on voltage of *m*-SiPhPPV is due to the higher energy barrier between the ITO and HOMO state of *m*-SiPhPPV, which results in a dramatic decrease of hole injection.

The current density increases exponentially with the increasing forward bias voltage, which is a typical diode characteristic. The dependence of luminance intensity of the *m*-SiPhPPV, *m*-SiPhPPV-*co*-MEH−PPV (75:25 wt %), and MEH−PPV diodes against voltage is also shown in Figure 3. The luminance intensity of MEH−PPV and *m*-SiPhPPV-*co*-MEHPPV (75:25 wt %) exponentially

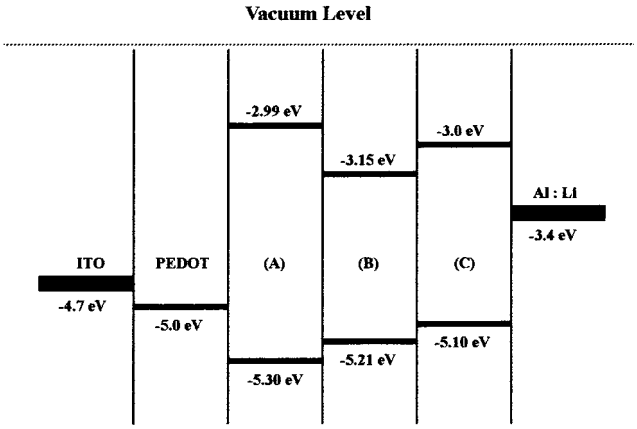

Figure 2. Hypothesized energy diagram of ITO/PEDOT/polymer/Al:Li devices *m*-SiPhPPV (A), *m*-SiPhPPV-*co*-MEH−PPV (75:25 wt %) (B), and MEH−PPV (C).

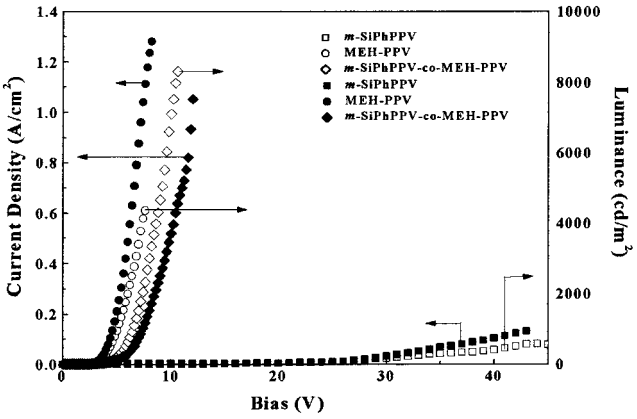

Figure 3. Current−voltage−luminance characteristics of ITO/PEDOT/polymer/Al:Li devices *m*-SiPhPPV, *m*-SiPhPPV-*co*-MEH−PPV (75:25 wt %), and MEH−PPV.

increased with an increased voltage. The linear dependence of the luminance intensity on the current density clearly indicated that charge carriers were easily injected from the electrodes by increasing the voltage. It is expected that the luminance power efficiency of the *m*-SiPhPPV-*co*-MEH−PPV (75:25 wt %) is higher than that of *m*-SiPhPPV or MEH−PPV because electrons are more easily injected from the cathode. Thus, the injected charge carriers are balanced and excitons were easily formed. After the low molecular weight portion of the *m*-SiPhPPV was removed by molecular cutting experiments using the membrane dialysis technique, the GPC curve and emission peak are narrower than those of a virgin polymer. In addition, the turn-on voltage of the ITO/*m*-SiPhPPV/Al:Li device is dramatically decreased as shown in Figure 4. This may be because it is a more homogeneous polymer and has a narrower emission wavelength after removal of the shoulder curve in GPC of the low molecular weight portion. The effect of the molecular cutting experiment is under investigation. Figure 5 shows the EL spectra of an ITO/PEDOT (25 nm)/polymer (120 nm)/Al:Li (100 nm) device. The EL spectrum peaks of the *m*-SiPhPPV, *m*-SiPhPPV-*co*-MEH−PPV (75:25 wt %), and MEH−PPV are almost identical to that of the PL spectrum (see Figure 1). These results suggest that the mechanism of PL and EL emission is due to the same excited singlet exciton state. Figure 6 shows the luminance intensity versus

(28) Chen, E. K.; Meng, H.; Lai, Y. H.; Huang, W. *Macromolecules* **1999**, *32*, 4351.

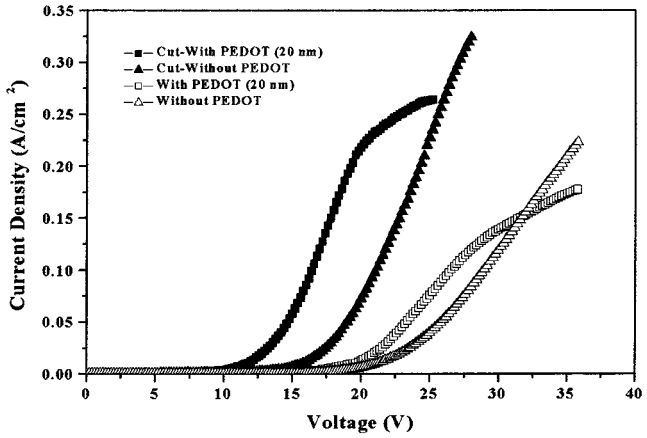

Figure 4. Current−voltage characteristics of ITO/(PEDOT)/*m*-SiPhPPV/Al:Li devices before and after molecular cutting experiments.

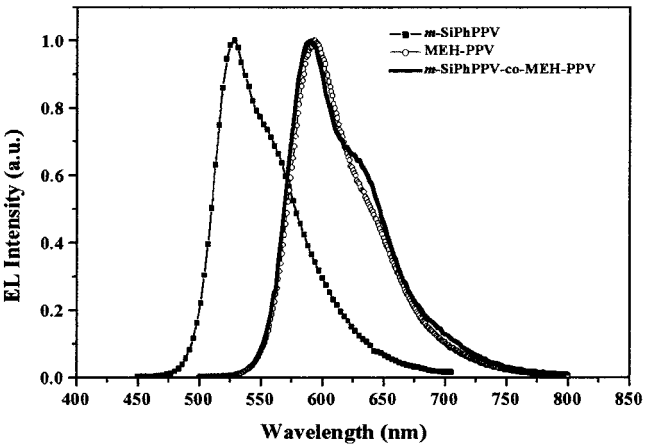

Figure 5. Electroluminescent spectra of ITO/PEDOT/polymer/Al:Li devices *m*-SiPhPPV, *m*-SiPhPPV-*co*-MEH−PPV (75:25 wt %), and MEH−PPV.

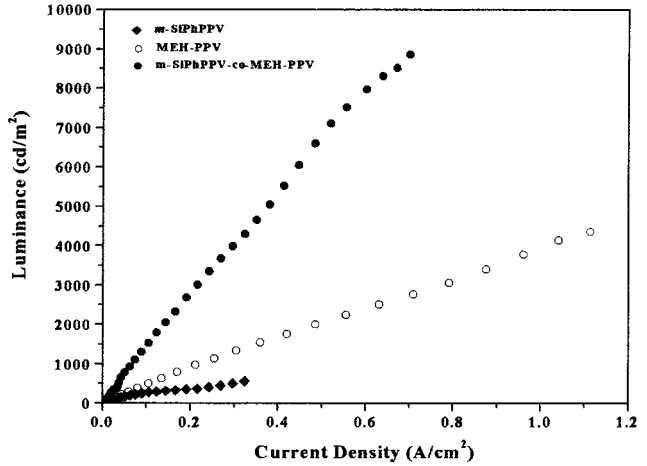

Figure 6. Dependence of luminance intensity on injection current of ITO/PEDOT/polymer/Al:Li devices *m*-SiPhPPV, *m*-SiPhPPV-*co*-MEH−PPV (75:25 wt %), and MEH−PPV.

current density characteristics of the ITO/PEDOT/polymer/Al:Li device. This is a good indication that the emission is due to the recombination of charge carriers injected from both electrodes into the emitting polymer layers to form singlet excitons. The copolymer, *m*-SiPhPPV-*co*-MEH−PPV (75:25 wt %), shows higher luminance intensity compared to *m*-SiPhPPV and MEH−PPV. The device performance characteristics of the single-layer devices are summarized in Table 3. The EL maximum peak of *m*-SiPhPPV-*co*-MEH−PPV (75:25 wt %) is about 67 nm red-shifted relative to that of *m*-SiPhPPV. The maximum brightness of the *m*-SiPhPPV-*co*-MEH−PPV (75:25 wt %) is about 19 180 cd/m^2 at 12.6 V with a current density of about 1.06 A/cm^2. Figure 7 shows the luminance versus lifetime of the ITO/PEDOT/*m*-SiPhPPV-*co*-MEH−PPV (75:25 wt %)/Ca/Al device and ITO/PEDOT/MEH−PPV/Ca/Al device for comparison. The half lifetime of a single-layer device of *m*-SiPhPPV-*co*-MEH−PPV (75:25 wt %) at 1000 cd/m^2 is about 120 h in nitrogen at room temperature. However, the half lifetime of the MEH−PPV device rapidly decreased at 7 h. To overcome the initial decrease in the luminance and to prolong the device's lifetime, we are now investigating the optimum device configuration. The maximum luminance efficiency was 2.9 lm/W with 10 mA/cm^2 at 9.6 V.

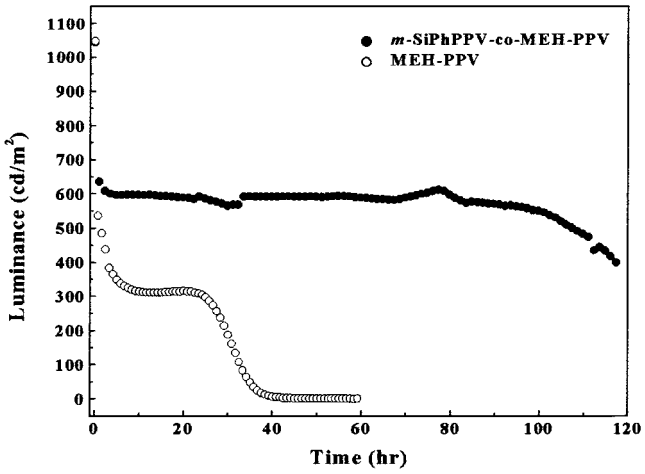

Figure 7. Luminescence versus lifetime of ITO/PEDOT/*m*-SiPhPPV-*co*-MEH−PPV (75:25 wt %)/Ca/Al and ITO/PEDOT/MEH−PPV/Ca/Al devices in air at room temperature.

Table 3. Device Performance Characteristics of the Resulting Polymers in ITO/PEDOT/Polymer/Al:Li Devices

polymer	turn-on voltage	maximun luminous efficiency (lm/W)	maximum luminance (cd/m^2)
m-SiPhPPV	14	0.08	570 (43 V)
m-SiPhPV-*co*-MEH−PPV (90:10 wt %)	5.5	0.74	4920 (18 V)
m-SiPhPV-*co*-MEH−PPV (75:25 wt %)	2.3	2.9	19180 (12 V)
m-SiPhPV-*co*-MEH−PPV (20:80 wt %)	1.9	1.74	17200 (10.5 V)
MEH−PPV	2.0	0.89	4450 (7.8 V)

Conclusions

This study focused on the design of molecular architecture and the synthesis of asymmetric poly(*p*-phenylene vinylene) derivatives for polymer light-emitting diodes to allow both the processibility and the emission colors to be changed from green to orange-red and the purification of the resulting polymers by membrane dialysis to improve the device's performance. The *m*-SiPhPPV and copolymers with high molecular weights were completely soluble in common organic solvents and could be spun cast onto the ITO glass substrate because

of the introduction of a bent-type dimethyldodecylsilylphenyl substitutent in the PPV's backbone. The external PL quantum efficiencies of MEH−PPV and *m*-SiPhPPV-*co*-MEH−PPV (75:25 wt %) were about 18% and 21 ± 2%, respectively. The emission color of the copolymers was red-shifted with a small amount of MEH−PPV. The copolymers showed higher luminescence efficiency compared to the *m*-SiPhPPV and MEH−PPV. EL devices of ITO/PEDOT/*m*-SiPhPPV-*co*-MEH-PPV (75:25 wt %)/Al:Li exhibited a luminance efficiency of up to 2.9 lm/W and maximum brightness of up to 19 180 cd/m^2. Lifetime stability of the ITO/PEDOT/*m*-SiPhPPV-*co*-MEHPPV (75:25 wt %)/Ca/Al device at 1000 cd/m^2 is about 120 h and higher than that of MEH−PPV in a nitrogen atmosphere at constant dc mode. From these results, copolymer systems are the most promising emitting materials for use in a polymeric electroluminescence display.

Acknowledgment. This work was supported by the Korea Research Foundation Grant (KRF-2000-003-D00100).

CM010593S